THE JOURNAL OF BIOLOGICAL CHEMISTRY VOL. 287, NO. 22, pp. 18769–18780, May 25, 2012

Liver-specific p70 S6 Kinase Depletion Protects against Hepatic Steatosis and Systemic Insulin Resistance*[S]

Received for publication, March 23, 2012 Published, JBC Papers in Press, April 9, 2012, DOI 10.1074/jbc.M112.365544

Eun Ju Bae[‡1,2], Jianfeng Xu[‡1], Da Young Oh[‡], Gautam Bandyopadhyay[‡], William S. Lagakos[‡], Malik Keshwani[§], and Jerrold M. Olefsky[‡3]

From the Departments of [‡]Medicine and [§]Pharmacology, University of California, San Diego, California 92093

Background: In obesity/type 2 diabetes, stimulation of lipogenesis is sensitive to insulin, whereas, insulin's effect to suppress glucose production is impaired.
Results: Liver-specific p70 S6K knockdown in HFD mice improved systemic insulin sensitivity, and attenuated liver steatosis and *de novo* lipogenesis.
Conclusions: S6K is an important component of selective hepatic insulin resistance.
Significance: Hepatic p70 S6K may be a potential therapeutic target in metabolic diseases.

Obesity-associated hepatic steatosis is a manifestation of selective insulin resistance whereby lipogenesis remains sensitive to insulin but the ability of insulin to suppress glucose production is impaired. We created a mouse model of liver-specific knockdown of p70 S6 kinase (S6K) (L-S6K-KD) by systemic delivery of an adeno-associated virus carrying a shRNA for S6K and examined the effects on steatosis and insulin resistance. High fat diet (HFD) fed L-S6K-KD mice showed improved glucose tolerance and systemic insulin sensitivity compared with controls, with no changes in food intake or body weight. The induction of lipogenic gene expression was attenuated in the L-S6K-KD mice with decreased sterol regulatory element-binding protein (SREBP)-1c expression and mature SREBP-1c protein, as well as decreased steatosis on HFD. Our results demonstrate the importance of S6K: 1) as a modulator of the hepatic response to fasting/refeeding, 2) in the development of steatosis, and 3) as a key node in selective hepatic insulin resistance in obese mice.

Most type 2 diabetic patients exhibit hepatic insulin resistance along with varying degrees of steatosis. In diabetes/obesity, hepatic insulin resistance can be selective; *i.e.* insulin's ability to inhibit gluconeogenesis is impaired, whereas insulin-stimulated lipogenesis is not (1). Insulin induces *de novo* lipogenesis by activating the key transcription factor SREBP-1c through a PI3K/Akt signaling pathway (2, 3). A recent study has shown that liver-specific insulin receptor knock-out mice exhibit global hepatic insulin resistance with no steatosis, confirming the key role of insulin signaling in fat accumulation in liver (4). This study suggests the presence of divergent intrahepatocyte insulin signaling pathways, allowing enhanced hepatic lipogenesis and gluconeogenesis in insulin-resistant states.

p70 S6 kinase (S6K)[4] is phosphorylated and activated by the upstream kinase mammalian target of rapamycin complex1 (mTORC1) in response to growth factors, insulin, or nutrients such as glucose and amino acids (5). Plasma levels of amino acids are elevated in obesity and amino acid infusion leads to insulin resistance (6). The activity of mTORC1 and S6K are increased in liver, skeletal muscle, and fat tissue in genetic and diet-induced obese animals and have been shown to modulate insulin sensitivity and obesity (7–9). The increased mTORC1/S6K activity leads to serine phosphorylation and protein degradation of IRS, creating a negative feedback loop in which insulin signaling can attenuate subsequent insulin action (10). The mTORC1 inhibitor rapamycin reverses this inhibitory effect, and deletion of S6K protects Akt from this negative feedback loop, further demonstrating that S6K can exert inhibitory effects on insulin signaling (11, 12).

Consistent with this observation, Um *et al.* showed that S6K1 knock-out mice were protected from diet-induced obesity and insulin resistance. However, in the context of obesity, the role of S6K in hepatic steatosis remains poorly understood. mTORC1, as a downstream target of Akt activation, stimulates lipogenesis (13, 14). Several amino acids such as glutamine, leucine, and alanine can stimulate lipogenesis in hepatocytes and this is cou-

* This work was supported, in whole or in part, by Grants DK033651, DK074868, T32 DK 007494, and DK063491 from the National Institutes of Health. This work was also supported by the Eunice Kennedy Shriver NICHD/National Institutes of Health through cooperative agreement U54 HD 012303-25 as part of the specialized Cooperative Centers Program in Reproduction and Infertility Research.
[S] This article contains supplemental Table S1 and Figs. S1–S5 and Experimental Procedures.
[1] Both authors contributed equally to this work.
[2] Present address: Woosuk University, 443 Samnye-ro, Samnye-eup, Wanjugun, Jeollabuk-do 565-701, Korea.
[3] To whom correspondence should be addressed: Division of Endocrinology & Metabolism, Department of Medicine, University of California, San Diego, 9500 Gilman Dr., La Jolla, CA 92093. Tel.: 858-534-6651; Fax: 858-534-6653; E-mail: jolefsky@ucsd.edu.

[4] The abbreviations used are: S6K, p70 S6 kinase; L-S6K-KD, liver-specific S6K1/2 knockdown; NC, normal chow; HFD, high fat diet; SREBP, sterol regulatory element-binding protein; mTORC1, mammalian target of rapamycin complex1; 4E-BP, 4E-binding proteins; AAV, adeno-associated virus; shRNA, small hairpin RNA; siRNA, small interfering RNA; GTT, glucose tolerance tests; ITT, insulin tolerance tests; FFA, free fatty acids; GDR, the rate of glucose disappearance; GIR, glucose infusion rate; HGP, hepatic glucose production; PEPCK, phosphoenolpyruvate carboxykinase; FOXO1, forkhead box O1; GSK3, glycogen synthase kinase 3; MCR-I, metabolic clearance rate of insulin; PGC1α, PPAR$\gamma\gamma$coactivator 1α; SCD1, stearoyl coenzyme A desaturase 1; FAS, fatty acid synthase.

pled to S6K activation (15). In addition, genetic knock-out of eukaryotic translation initiation factor 4E-binding proteins (4E-BPs), 4E-BP1/2, which are two major downstream targets of mTORC1, leads to increased S6K activity with increased susceptibility to HFD-induced obesity, fatty liver, and insulin resistance (16). Moreover, inhibition of mTORC1 can attenuate insulin induction of the SREBP-1c-dependent lipogenic program and liver steatosis in mice (17–19).

To explore the pathophysiologic role of S6K in steatosis and selective hepatic insulin resistance, we established liver-specifc S6K knockdown mice using systemic delivery of adeno-associated virus (AAV) expressing small hairpin RNA (shRNA) targeted against S6K1/2. In this study, we show that depletion of hepatic S6K protects mice from HFD-induced systemic insulin resistance by increasing insulin signaling not only in liver but also in fat and skeletal muscle. Furthermore, it suppresses SREBP-1c expression and *de novo* lipogenesis, resulting in ameliorated HFD-induced hepatosteatosis.

EXPERIMENTAL PROCEDURES

Animals and AAV Treatment—Male C57BL/6 mice were purchased from Harlan Laboratories (Blue Mounds, WI). The AAV vector plasmid was constructed by insertion of the shRNA expression cassette fragment from the backbone of pSilencer-H1 3.0 (Ambion, Austin, TX) and the recombinant AAV vectors were prepared according to Snyder *et al.* with minor modifications (20). Briefly, the AAV vector plasmid, adenoviral helper and AAV helper plasmid were transfected to subconfluent HEK293 cells using calcium phosphate. Three days after transfection, cells were lysed, and AAV viral particles were purified by CsCl gradient ultracentrifuge. Virus titer was determined by dot blot and 4×10^{11} genome copies were injected into 5-week-old mice. Mice were injected with either AAV encoding shRNA for S6K or a nonspecific sequence. siRNA targeting both S6K1 and S6K2 was synthesized as 21-nucleotide siRNA duplexes with two deoxythymidine bases corresponding to the S6K1/2 target sequence (5′-CTCAGTGAGAGTGCCAACCAA-3′). The control AAV encoding shRNA was a 20-nucleotide sequence (5′-ACTACCGTTGTATAGGTGTT-3′). After AAV injection, mice were maintained on either NC or HFD (60% kcal from fat; D12492, Research Diets). Animals were maintained on a 12 h light/dark cycle with free access to food and water. To determine insulin's effects on hepatic lipogenesis and gluconeogenesis, glucose clamp studies were performed on 5-month-old mice on 12 weeks 60% HFD and age matched NC fed mice as controls. The body weights were 27 g *versus* 50 g for the normal chow (NC) and HFD mice, and lean body mass was 19 g *versus* 27 g for NC *versus* HFD mice, respectively. Mouse procedures conformed to the Guide for Care and Use of Laboratory Animals of the US National Institutes of Health and were approved by the Animal Subjects Committee of the University of California, San Diego. For fasting/refeeding studies, mice were fasted overnight (21 h) and refed NC or HFD for 6 h prior to tissue harvest. Serum insulin levels were analyzed by ELISA (Alpco Diagnostics), and FFA levels were measured by enzymatic assay (Wako Diagnostics, VA).

Metabolic Studies—Glucose and insulin tolerance tests (GTT and ITT, respectively) were performed on 7 h fasted mice. Animals were injected intraperitoneally with either dextrose (1 g/kg, Hospira, Inc) or insulin (0.6 units/kg, Novolin R, Novo-Nordisk). Glucose excursion after injection was monitored over time. Blood samples were drawn by tail nick at basal and indicated times, and glucose was measured using a One-Touch glucose-monitoring system (Lifescan).

Hyperinsulinemic-Euglycemic Clamp—Hyperinsulinemic-euglycemic clamp studies were performed as previously described (21). In brief, two jugular catheters were inserted under anesthesia by ketamine, acepromazine, and xylazine administered via intramuscular injection. The catheters were tunneled to the mid-scapular region and externalized. The mice were allowed to recover for 5 days. The clamp experiments began with the infusion of an equilibration solution of D-[3-^{3}H]glucose (NEN, Boston) for 90 min at a constant rate of 5 μCi/h. Then, insulin was infused at 8 mU/kg/min while glucose infusion rate was increased or decreased as necessary until euglycemia was reached ($\sim$120 mg/dl for $>$20 min). Blood samples were collected prior to insulin infusion and upon euglycemia to confirm steady-state and assess free fatty acids (FFA) levels. At steady-state, the rate of glucose disappearance (total GDR) is equal to the sum of hepatic glucose production (HGP) and glucose infusion rate (GIR). The IS-GDR is equal to the total GDR minus the basal glucose turnover rate. The suppression of FFA is calculated by comparing plasma FFA concentrations in the basal and clamp states.

Triglyceride Measurement—TG content was measured in liver homogenates in PBS containing 5% Triton X-100 and plasma (EnzyChrom™, BioAssay Systems, Hayward, CA). TG content was also measured in eWAT tissues. An aliquot of 50 μl of eWAT homogenate was used for DNA extraction and relative genome copy number was determined by qPCR.

Histology and Oil Red O Staining—H&E staining in liver sections was conducted by the University of California, San Diego, histology core at Moore's Cancer Center. Frozen liver sections were used for Oil Red O staining to visualize neutral lipids.

Immunoprecipitation and Immunoblot Analysis—Snap-frozen liver, skeletal muscle, and white adipose tissue were lysed in lysis buffer containing 1% Nonidet P-40, NaCl, Tris, and phosphatase and protease inhibitors from Roche. The protein concentration was determined by BCA protein assay (Bio-Rad). For immunoprecipitations, lysates were incubated with 1 mg of anti-IRβ, IRS1 or IRS2 antibody (Santa Cruz Biotechnology) overnight at 4 °C and immune complexes were precipitated with protein A/G-conjugated beads (Invitrogen). Beads were washed with lysis buffer and resuspended in sample buffer. Lysates and immune complexes were separated by SDS-PAGE gel and subjected to Western blot. The separated proteins were transferred to polyvinylidene difluoride (PVDF) membranes (Bio-Rad), which were then washed with Tris/HCI, pH 7.4, containing 159 mM NaCl and 1% Tween 20 (TBS-T), and then blocked in 4% skim milk in TBS-T for 30 min. After washing with TBS-T, the membranes were probed with antibodies at 4 °C overnight. Immunoreactive protein bands were visualized with an ECL Western blot analysis system (Amersham Biosciences, Piscataway, NJ). Antibodies against S6K1, S6K2, IRS1, IRS2, IRβ, FAS, and SREBP-1 were from Santa Cruz Biotechnology. Antibodies against p-Akt (Ser473), p-mTOR (Ser2448),

p-S6K (Thr389), p-4E-BP1 (Thr37/46), p-FOXO1 (Ser256), p-S6 (Ser240/244), Akt, mTOR, and β-tubulin were obtained from Cell Signaling Technologies (Beverly, MA). Phosphotyrosine antibody (4G10®Platinum) was purchased from Upstate (Temecula, CA), and SCD1 from ALEXIS Biochemicals (San Diego, CA). ImageJ was used for quantification of the relative intensities of protein bands.

RNA Isolation and Quantitative RT-PCR—Total RNA was isolated from cells and tissues using TRIzol Reagent (Invitrogen, Carlsbad, CA) according to the manufacturer's instructions. First strand cDNA was synthesized using a High-Capacity cDNA Reverse Transcription Kit (Applied Biosystems, Foster City, CA). Gene expression levels were calculated after normalization to the standard housekeeping gene *RPS3* using the $\Delta\Delta C_T$ method as described previously (22). Primer sequences are available in supplemental Table S1.

Cell Culture, siRNA Transfection, and Adenoviral Infection—Primary hepatocytes were isolated from NC- or HFD-fed mice or from Sprague-Dawley rats by collagenase digestion. Primary hepatocytes were cultured in collagen-coated plates in serum free Dulbecco's Modified Eagle Medium (low glucose) and treated on the second day of isolation with reagents at indicated concentration and conditions.

p70 S6 Kinase Activity Assay—Steady-state kinetic assays were carried out for lysates catalyzed phosphorylation of the S6K model peptide substrate (Tide, RRRLSSLRA) according to the reference with small modifications (23). The 10-μl Tide phosphorylation reactions were performed at 25 °C in 40 mM MOPS buffer, pH 7, containing 0.1% 2-mercaptoethanol, 10 mm $MgCl_2$, and 0.2 mm sodium vanadate at fixed concentration of tide (200uM) and fixed concentrations of [γ-^{32}P]ATP(200 μM) for 30 min. The reaction was quenched using 30% acetic acid and 25 μl of quench reaction was spotted on p81 paper, washed three times for 10 min each in 75 mM phosphoric acid followed by 1 wash in acetone and air dried. The specific radioactivity of ^{32}P-radiolabeled Tide (^{SA}Tide, cpm/pmol) was determined from radioactivity detected by scintillation counting of the known amount of total Tide that was applied to the P81 paper; the micromolar amount of phosphorylated Tide product was determined by reference to the specific radioactivity of [γ-^{32}P]ATP (^{SA}ATP, ~1000–2000 cpm/pmol). The assays were performed in duplicates, and background was measured by removing the peptide from assay conditions.

Insulin Injection Study—After 7 h fasting, mice were injected with 1 units/kg insulin through inferior vena cava under anesthesia. Tissues were taken before or after injection (3 min for liver and 10 min for eWAT and muscle) and subjected to Western blot.

De Novo Lipogenesis Study—Liver *de novo* lipogenesis assay was done as described with some modifications (24). Briefly, mice were fast for 24 h, and 2 h before sacrifice, ^3H_2O was injected intraperitoneal in a dose of 3mCi/kg. About 0.5 g of liver tissues were saponificated with 1.5 ml of 30% KOH and 1.5 ml EtOH at 70 °C for 40 min, and then acidify by adding 1.5 ml of 9 M of H_2SO_4. Extractions by 5 ml of hexane for three times were combined, air-dried and counted to determine levels of ^{3}H-labeled fatty acids.

Data Analysis—Experimental results are expressed as means ± S.E. Results were tested for statistical significance by one way ANOVA or an unpaired, two-tailed Student's *t* test. The criterion for statistical significance was set at $p < 0.05$. Values are expressed as means ± S.E., and an asterisk mark indicates $p < 0.05$ unless otherwise clarified. Densitometry was performed using ImageJ software.

RESULTS

Mixed Insulin Resistance for Gluconeogenesis and Lipogenesis in HFD Mouse Liver—To determine the regulations of lipogenic and gluconeogenic pathway by insulin in normal and obese/insulin resistance stage, mRNA levels of a master lipogenic transcription factor SREBP-1c and the key gluconeogenic enzyme phosphoenolpyruvate carboxykinase (PEPCK) were measured in NC and HFD mouse liver at the end of a 3 h insulin infusion during hyperinsulinemic-euglycemic clamp studies. As expected, during the insulin infusion, PEPCK expression was suppressed by 65% in NC, whereas in HFD mice suppression was not observed, indicating the presence of hepatic insulin resistance for the gluconeogenesis pathway (Fig. 1, *A* and *B*). Basal expression of SREBP-1c was higher in HFD/obese mice. More interestingly, insulin administration increased SREBP-1c in both NC and HFD mice, with a similar degree of induction of 150 and 170%, respectively (Fig. 1*A*). A similar induction pattern was found in lipogenic gene fatty acid synthase (FAS, supplemental Fig. S1). This finding has not previously been reported and demonstrates the preservation of insulin sensitivity for the lipogenic pathway (Fig. 1*B*). Since circulating insulin levels are higher in HFD/obesity compared with NC lean controls, this indicates that *in vivo* lipogenic signaling is greater in HFD/obese mice, consistent with the increased basal SREBP-1c levels. To identify molecular correlates of the selective insulin sensitive lipogenic action, we measured the effect of insulin on various insulin signaling molecules in hepatocytes from NC or HFD mice. Akt phosphorylation was increased by insulin treatment at 15 and 30 min in hepatocytes from NC, but this effect was blunted in hepatocytes from HFD mice (Fig. 1*C*). Accordingly, phosphorylation of forkhead box O1 (FOXO1) and glycogen synthase kinase 3 (GSK3) β, which are downstream substrates of Akt, were also decreased in hepatocytes from HFD mice. In contrast to Akt phosphorylation, insulin stimulation of mTORC1 and S6K phosphorylation was not decreased in HFD compared with NC hepatocytes (Fig. 1*C*). Indeed, S6K kinase activity, as measured by Ser240/244 phosphorylation of S6 (Fig. 1*C*) and *in vitro* kinase assay (Fig. 1*D*), was enhanced in HFD hepatocytes in both basal and insulin-stimulated states. Finally, an elevated level of hepatic *de novo* lipogenesis in basal stage and during refeeding period *was* determined by incorporation of radioactivity from ^3H_2O to lipid fraction, consistent with SREBP-1c expression in HFD mice (Fig. 1*E* and supplemental Fig. S5*A*).

Glucose Homeostasis in Lean L-S6K-KD Mice—A siRNA sequence targeting both S6K1 and S6K2 was used to generate an AAV viral vector (25), and mice administered with this AAV are referred to as L-S6K-KD to note the selective knockdown of S6K in liver.

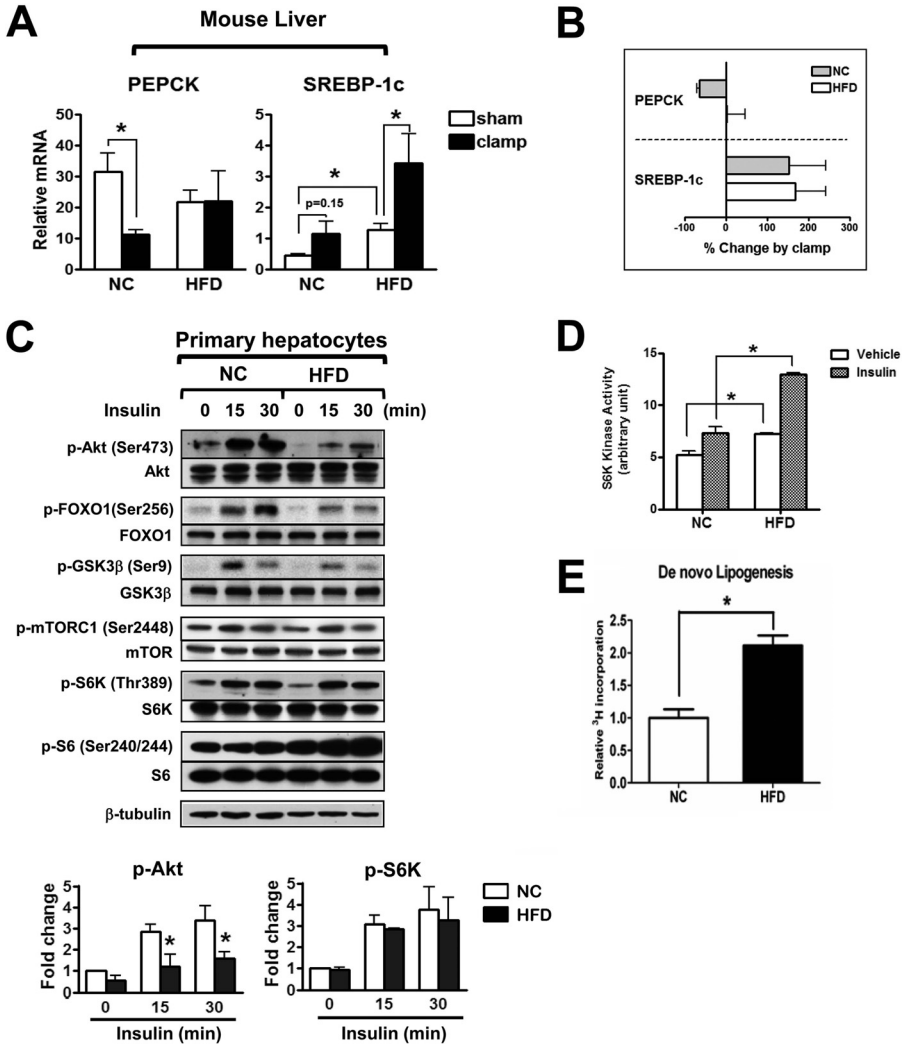

FIGURE 1. **Mixed insulin resistance for gluconeogenesis and lipogenesis in HFD mouse liver.** *A*, hepatic expression of PEPCK and SREBP-1c as measured by qPCR in NC or HFD mice after hyperinsulinemic-euglycemic clamp or sham-treatment. Mice were fed HFD for 10 weeks or maintained on NC. Clamp was done according to the method described in the supplemental Experimental Procedures, and liver was collected about 3 h after starting clamp for gene expression analysis. $n = 3$. *B*, gene expression changes in clamped mice relative to sham. *C*, immunoblot analyses of primary hepatocytes from NC or HFD mice before or after incubation with 100 nM insulin. *Upper panel* is a representative image from three independent experiments, and quantification of relative p-Akt and p-S6K is shown on the bottom. *D*, S6K kinase activity of hepatocytes from NC or HFD mice treated with vehicle or 100 nM insulin. *E*, hepatic *de novo* lipogenesis activity measured in NC and HFD mice.

Ten days after injection, mice from the control and L-S6K-KD groups were sacrificed and S6K expression was measured in various tissues. S6K1 and S6K2 protein levels were reduced by ~70% in liver after AAV-shRNA S6K administration, with no decrease in other tissues, including fat and skeletal muscle (Fig. 2*A*). Similar degrees of suppression were observed 5-week (Fig. 2*B*) and 4-month (Fig. 2*C*) after AAV injection, demonstrating liver-specific long-term AAV-mediated gene depletion.

An intra-peritoneal GTT was performed 4 weeks after AAV-shRNA S6K administration. As seen in Fig. 2*D*, basal blood glucose level was lower in L-S6K-KD mice with substantial improvement in glucose tolerance. The basal plasma insulin levels were lower in the L-S6K-KD mice while the 10 min levels were not significantly different (Fig. 2*E*). Interestingly, basal C-peptide levels were similar in the L-S6K-KD mice, whereas, the insulin to C-peptide ratio was reduced (supplemental Fig. S2*A*), implying that these mice display similar insulin secretion but enhanced insulin clearance.

Improved Glucose Homeostasis and Systemic Insulin Sensitivity in Obese/HFD L-S6K-KD Mice—To assess the effect of S6K depletion on obesity-induced insulin resistance, 8-week-old L-S6K-KD mice were fed HFD for 12 weeks. During HFD feeding, body weight gain (Fig. 3*A*) and average food intake remained the same as in control mice. After 10 weeks HFD, GTTs (Fig. 3*B*) and ITT (Fig. 3*C*) demonstrated improved glucose tolerance and an enhanced hypoglycemic effect of insulin in the L-S6K-KD mice. Basal plasma insulin levels after a 7 h fast were lower in the L-S6K-KD mice (Fig. 3*D*), indicative of increased insulin sensitivity, as in the NC fed mice.

We next performed hyperinsulinemic-euglycemic glucose clamp studies to quantitatively assess *in vivo* insulin sensitivity in the L-S6K-KD and control mice. As summarized in Fig. 4, *A–E*, the glucose infusion rate (GIR) required to maintain eug-

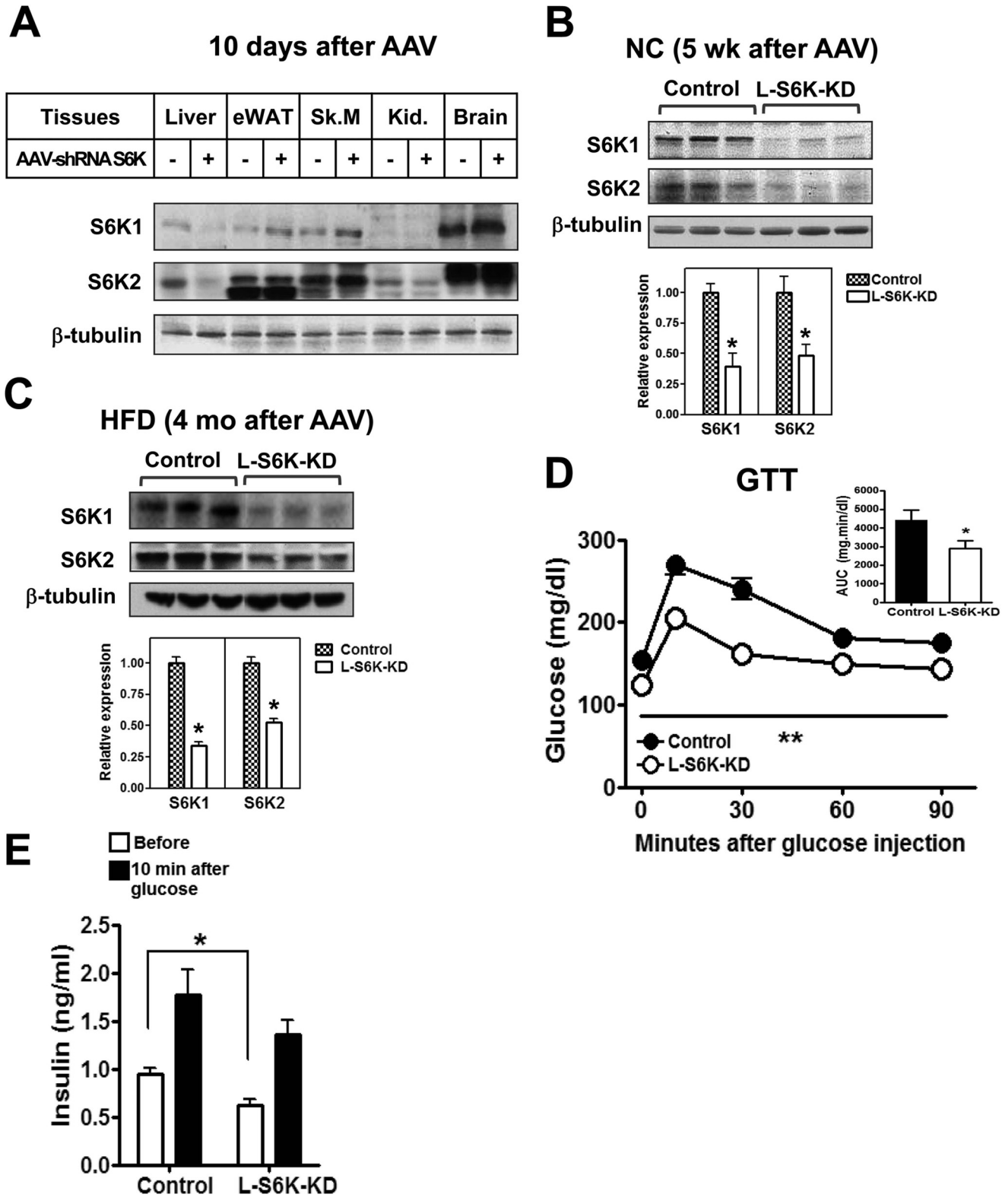

FIGURE 2. **Generation of L-S6K-KD mice and metabolic studies in NC fed mice.** *A*, immunoblot analyses of various tissues 10 days after intravenous injection of AAV-shRNA of control (−) or S6K (+). eWAT (*epididymal white adipose tissue*), Sk.M (*skeletal muscle*), Kid. (*kidney*). *B*, representative immunoblot analyses (*top*) and quantification (*bottom*) for S6K1 and S6K2 in livers of NC-fed mice 5 weeks after AAV-shRNA injection. $n = 6$. *C*, representative immunoblot (*top*) and quantification (*bottom*) for S6K1 and S6K2 in liver of HFD-fed mice. $n = 10–15$. *D*, GTTs in NC-fed mice. Area under the curve (AUC) from GTT is shown in *inset*. $n = 6–8$, **, $p < 0.01$ *versus* control. *E*, serum insulin levels in NC-fed mice. Serum collected before and 10 min after intraperitoneal injection of glucose was used for the measurement of insulin level.

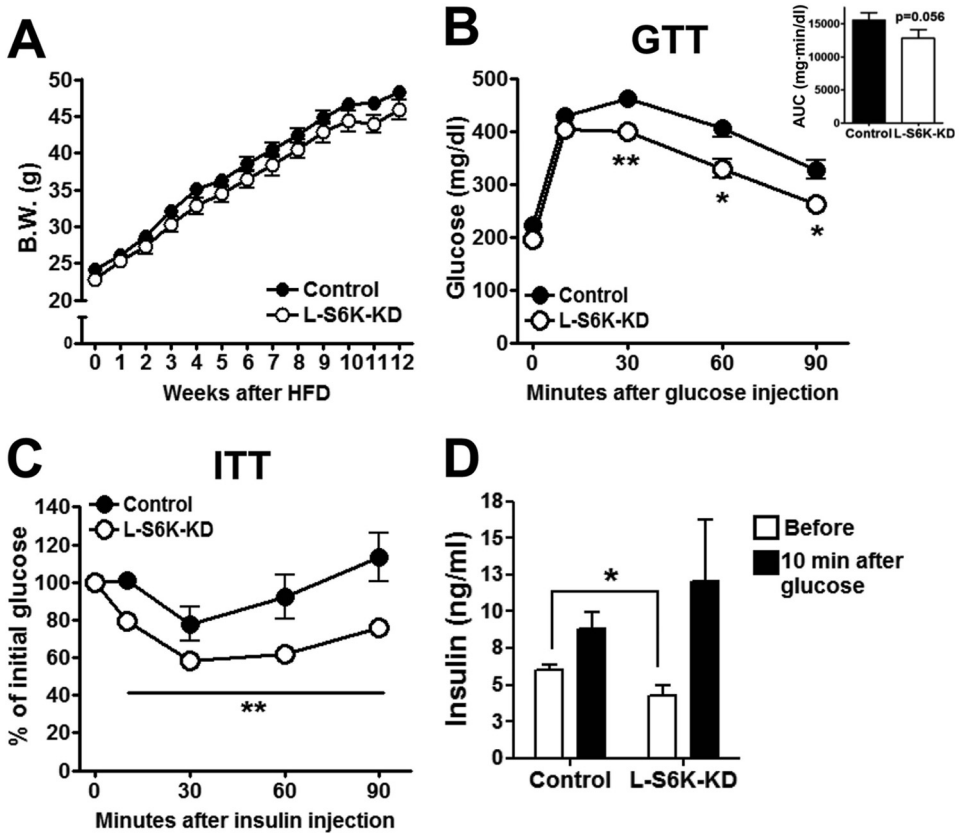

FIGURE 3. **Improvement of glucose homeostasis in L-S6K-KD HFD-fed mice.** L-S6K-KD mice were put on 60% HFD from 8 weeks of age for 16 weeks. *A*, growth curves upon HFD feeding up to 12 weeks. Body weights were measured every week. $n = 10–15$ mice per group. *B*, GTT was performed in HFD-fed control or L-S6K-KD mice as described in Fig. 2*D*. AUC of blood glucose is shown in the insert. $n = 7–10$ per group. *, $p < 0.05$ and **, $p < 0.01$ *versus* control. *C*, ITT in HFD-fed control or L-S6K-KD mice. Insulin (0.6 units/kg) was intraperitoneally injected to 7 h fasted HFD mice, and blood glucose was measured at the indicated time points. Data are expressed as percentage change from baseline. Each *circle* represents the means ± S.E. from 6 mice. **, $p < 0.01$ *versus* control. *D*, serum insulin levels in HFD mice. The same mice used in *B* were fasted for 7 h 1 week after GTT. Glucose (1 g/kg) was given by oral gavage and blood was collected after 10 min for insulin ELISA.

lycemia, as well as the insulin-stimulated glucose disposal rate (IS-GDR) was increased in L-S6K-KD HFD mice (Fig. 4, *A* and *B*). Since 70–80% of IS-GDR is attributable to skeletal muscle glucose uptake, these results indicate that L-S6K-KD leads to improved skeletal muscle insulin sensitivity. Basal rates of hepatic glucose production (HGP) were not changed in L-S6K-KD mice (Fig. 4*C*) and since basal HGP is the major contributor to fasting hyperglycemia, these results are consistent with the minimal changes in basal glucose levels in these animals (Fig. 3*B*). However, we found that the ability of insulin to suppress HGP was enhanced in L-S6K-KD HFD mice (Fig. 4*D*), as was the suppression of FFA (Fig. 4*E*). Consistent with this, the effect of insulin injection to stimulate liver and adipose tissue Akt phosphorylation was increased in the L-S6K-KD mice (Fig. 4*F*). Steady-state glucose and insulin levels during the clamp studies are provided in supplemental Fig. S2*B*, and interestingly, the metabolic clearance rate of insulin (MCR-I), calculated from the steady-state insulin concentration during the clamp studies, was greater in L-S6K-KD HFD mice (Fig. 4*G*). Since the steady-state insulin levels were ~25% lower in the L-S6K-KD HFD mice, this suggests that the magnitude of the increased insulin sensitivity in these animals is somewhat underestimated in Fig. 4, *A–E*. Taken together, the *in vivo* results support the conclusion that L-S6K-KD HFD mice exhibit enhanced systemic insulin sensitivity, affecting skeletal muscle and adipose tissue, as well as liver.

Enhanced Hepatic Insulin Signaling in L-S6K-KD HFD Mice—To determine the mechanisms for enhanced insulin sensitivity in L-S6K-KD HFD fed mice, we assessed the insulin signaling pathway in tissues from these mice. To induce endogenous insulin stimulation, samples were taken from overnight fasted and 6 h refed mice. After 6-hour refeeding, IRβ or IRS1/2 tyrosine phosphorylation showed little, if any changes in HFD control mice compared with those in fasted mice, whereas phosphorylation was increased in L-S6K-KD mice (Fig. 5*A*). This could be due to an increased rate of phosphorylation or decreased dephosphorylation in the L-S6K-KD mice. Total expression level of IR β was not changed by S6K deletion in liver, whereas IRS1 protein decreased and IRS2 protein increased (Fig. 5, *A* and *B*). Although it has been shown that phosphorylation of IRS-1 Ser307 was decreased in S6K1 depleted Hela cells (7), this was not affected by S6K knock down in our model. Since plasma insulin levels after refeeding were comparable between the groups (data not shown), the *in vivo* signaling results indicate increased insulin sensitivity in L-S6K-KD animals.

Refeeding led to stimulation of Akt phosphorylation in L-S6K-KD mice, whereas, this effect was severely blunted in the

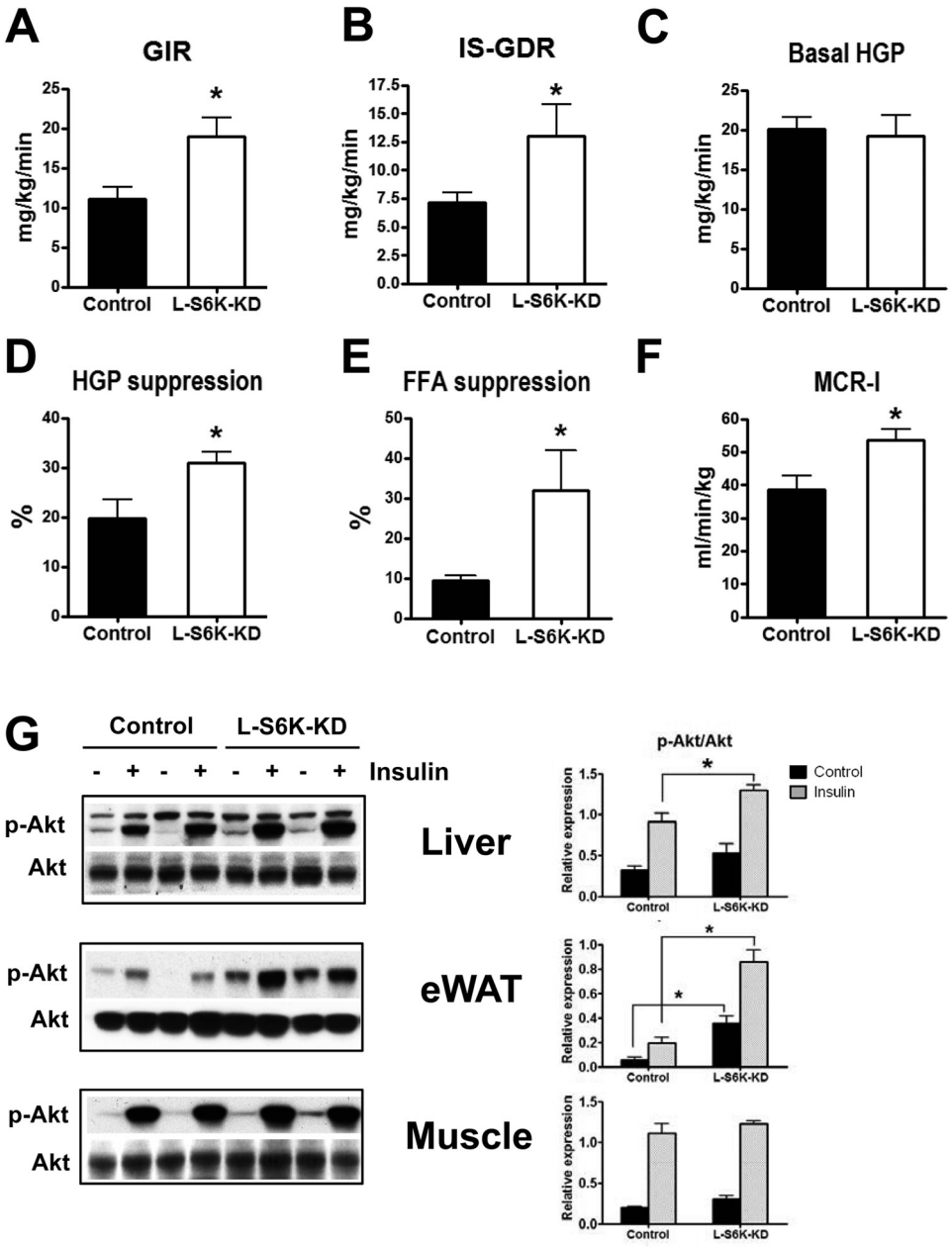

FIGURE 4. **Improved *in vivo* insulin sensitivity determined by hyperinsulinemic-euglycemic clamp and acute insulin injection in L-S6K-KD HFD-fed mice.** *In vivo* insulin sensitivity as determined by hyperinsulinemic-euglycemic clamp in control ($n = 7$) and L-S6K-KD ($n = 5$) mice fed HFD. GIR (*A*), IS-GDR (*B*), Basal HGP (*C*), suppression of HGP (*D*), suppression of plasma FFA (*E*), and metabolic clearance rate of insulin (MCR-I) (*F*), are presented as means ± S.E. *G*, immunoblot analysis of Akt Ser473 phosphorylation in liver, eWAT and skeletal muscle from HFD control and L-S6K-KD mice after acute insulin injection (1 units/kg). Liver was harvested in 3 min after insulin injection and eWAT and skeletal muscle in 10 min. A representative blot (*left*) and quantification results (*right*) are shown.

control HFD mice (Fig. 5*C*). Furthermore, the downstream targets of Akt, GSK3β, and FOXO1, showed the same pattern. However, refeeding did lead to a significant increase in mTORC1 phosphorylation (S2448), and this effect was enhanced in the HFD L-S6K-KD mice, indicating nutrients can be an additional input to mTORC1 activation. As expected, phosphorylation of S6 protein was greatly reduced when hepatic S6K was knockdown. As shown in supplemental Fig. S3, *A* and *B*, refeeding also stimulated Akt phosphorylation in adipose tissue and muscle and this effect was increased in L-S6K-KD mice.

S6K Knockdown in Liver Reduces Hepatic Lipid Content and Lipogenesis—Although the role of S6K in glucose homeostasis has received considerable attention, its effects on lipid metabolism are poorly understood. H/E staining showed decreased steatosis and decreased fat content was confirmed by Oil Red O staining (Fig. 6*A* and quantified in 6B *bottom right*). Total liver weight normalized to body weight was significantly lower in L-S6K-KD HFD mice (Fig. 6*B*, *top left*), and this decrease in liver weight was associated with decreased liver TG content (Fig. 6*B*, *bottom left*). Plasma TG levels were also decreased in the L-S6K-KD mice (Fig. 6*B*, *top right*). In contrast to reduced liver

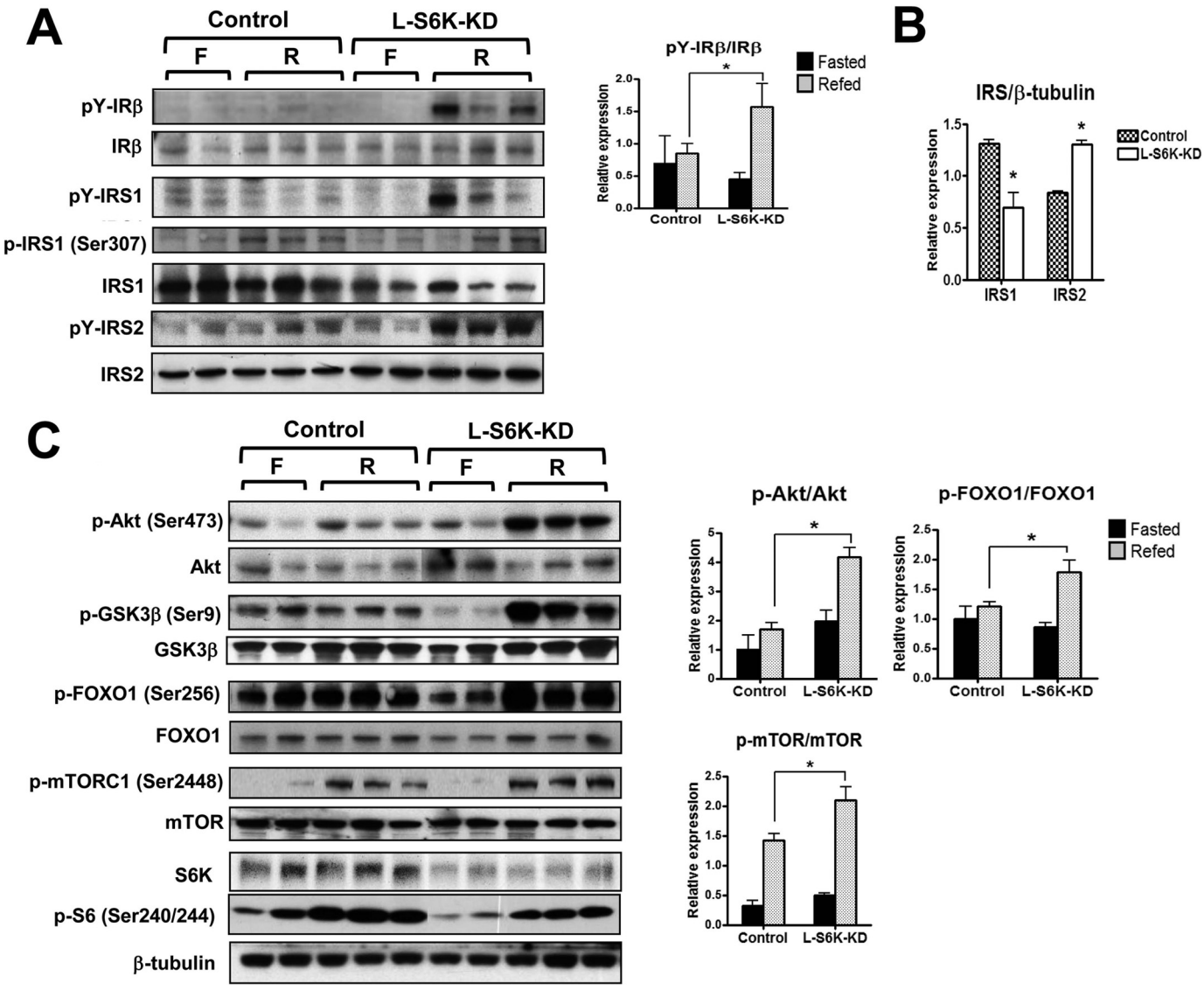

FIGURE 5. **Insulin signaling in liver after fasting (*F*)/refeeding (*R*) of HFD-fed control or L-S6K-KD mice.** Mice were either fasted for 21 h or refed HFD for 6 h after 15 h fasting and the liver was collected for analysis. The immunoblot analyses were done in 4–6 mice, and a representative blot (*left*) and quantification results (*right*) are shown. *A*, immunoblot analyses in liver for phosphorylation and total expression of IRβ and IRS1/2. A representative blot (*left*) and the quantification results of tyrosine phosphorylation normalized to total IR (*right*). *B*, quantification results of IRS1 and IRS2. Each bar represents the means ± S.E. of expression level of IRS1 and IRS2 from 10 mice per group. *, $p < 0.05$ *versus* control. *C*, immunoblot analyses in liver tissue lysates from HFD control and L-S6K-KD mice after fasting or refeeding. A representative blot (*left*) and quantification results (*right*) are shown.

weight in L-S6K-KD HFD mice, refeeding led to a greater increase in adipose mass in these mice (supplemental Fig. S4) compared with controls, indicating a differential distribution of fat between liver and adipose tissue.

Overnight fasting followed by 6-hour HFD refeeding significantly increased expression of SREBP-1c, fatty acid synthase (FAS) and acetyl-CoA carboxylase (ACC) in control HFD mice (Fig. 7*A*), consistent with the preserved hepatic effect of insulin on SREBP-1c induction in these animals (Fig. 1*A*). Refeeding stimulation of FAS and ACC mRNA levels also tended to be lower in L-S6K-KD HFD mice, but did not reach statistical significance, probably due to the smaller induction fold on HFD after 6 h of refeeding than NC feeding (supplemental Fig. S5*B*). However, the protein levels of FAS and steryol CoA desaturase1 (SCD1) were significantly decreased in the S6K knockdown group (Fig. 7*B*). Furthermore, in chow-fed animals, the fasting/refeeding paradigm led to marked increases in SREBP-1c, FAS, and SCD1 mRNA expression and all of these changes were significantly blunted in the L-S6K-KD mice (Fig. 7*C*). Signaling from the LXRα nuclear hormone receptor can increase SREBP-1c levels, but LXRα expression was unchanged between the genotypes (Fig. 7*A*). In NC-fed mice, liver-specific S6K KD also led to less induction of SREBP-1c protein expression, upon refeeding (Fig. 7*D*). As a more physiologic measure of hepatic lipid metabolism, hepatic *de novo* lipogenesis was assessed by measuring incorporation of radioactivity from ^3H_2O to the lipid fraction. The fasting/refeeding protocol efficiently stimulated lipogenic activity in controls, and this effect was attenuated by ~33% in L-S6K-KD mice (Fig. 7*E*).

These data clearly show that hepatic S6K depletion leads to a decrease in the lipogenic program in HFD/obese mice and also attenuates the refeeding effect to augment SREBP-1c, its down-

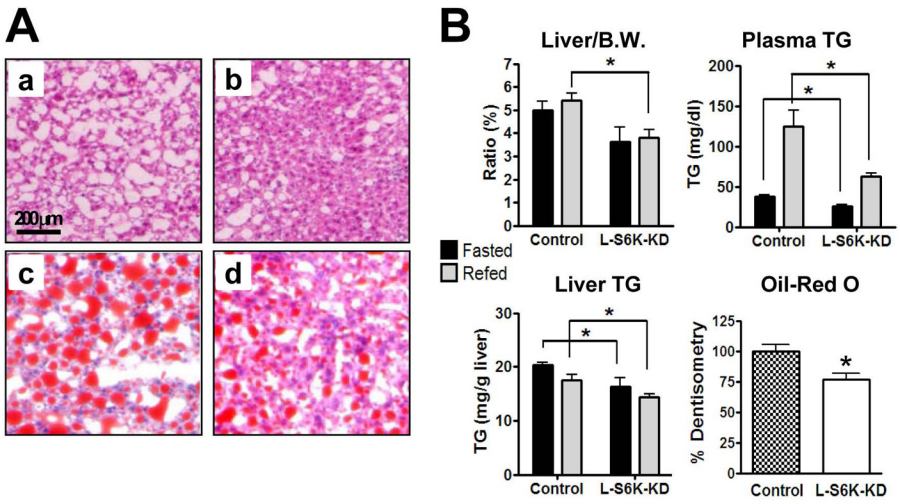

FIGURE 6. **HFD-induced hepatic steatosis is ameliorated in L-S6K-KD mice.** *A*, representative microphotographs of H&E (*a*, *b*) and Oil Red O staining (*c*, *d*) in liver of HFD-fed control (*a*, *c*) and L-S6K-KD (*b*, *d*) mice. *B*, liver weight, plasma TG, liver TG, and quantification of liver Oil Red O staining of HFD-fed control or L-S6K-KD mice after fasting/refeeding as described in the legend to Fig. 5. $n = 4–6$ mice per group.

stream target genes, and the biologic process of *de novo* lipogenesis. To assess the mechanisms of this S6K effect and to determine whether this is direct or indirect, we conducted *in vitro* experiments in isolated rat hepatocytes with and without the mTORC1 inhibitor, rapamycin, or the S6 kinase inhibitor, PF-4708671 (Fig. 7, *F* and *G*). Rapamycin treatment produced a marked decrease in SREBP-1c expression, consistent with earlier reports (17), and since mTORC1 is upstream of S6K and 4E-BP1, there was also a decrease in S6K, S6, and 4E-BP1 phosphorylation. Interestingly, PF4708671 effectively blocked S6K activity, but was without affect on SREBP-1c levels (Fig. 7, *F* and *G*).

DISCUSSION

Although the concept of mixed, or selective, hepatic insulin resistance in obesity has received recent attention, the main evidence for this concept has been the ongoing state of heightened lipogenesis at the same time as insulin's effects to inhibit gluconeogenesis are impaired. However, to our knowledge, it has not been demonstrated that insulin stimulation of hepatic lipogenesis is preserved, or enhanced, in the HFD/obese state. In the current studies, we directly show that the degree of hepatic SREBP-1c induction by the insulin infusion during the euglycemic clamp study was comparable between NC and HFD mice, demonstrating that the lipogenic pathway remains fully sensitive to insulin, despite HFD/obesity and systemic insulin resistance. In contrast, PEPCK suppression was negligible in HFD compared with NC mice, supporting the concept of selective or mixed hepatic insulin resistance for gluconeogenesis *versus* lipogenesis. Consistent with this, 6 h refeeding increased SREBP-1c mRNA 4-fold, whereas, it failed to suppress PEPCK or glucose-6-phosphatase (G6Pase) mRNA expression (data not shown) in the HFD refeeding study. We also found that insulin treatment stimulated S6K activity to a greater degree in hepatocytes from HFD compared with NC mice, whereas other aspects of insulin signaling were blunted by HFD. This effect of insulin to activate S6K in HFD mice is consistent with the heightened induction of SREBP-1c, lipogenic enzymes and *de novo* lipogenesis in the obese/insulin resistant state.

In these studies, we found that AAV-shS6K administration led to substantial and long lasting depletion of hepatic S6K. This is consistent with the view that AAVs preserve episomal forms or integrate into the genome, producing continued expression of the shRNA, leading to essentially permanent reduction of gene expression (20). Since S6K can be activated by insulin, creating a negative feedback loop by inhibiting IRS through serine phosphorylation and reducing insulin sensitivity, the amelioration of insulin resistance by S6K knockdown makes mechanistic sense. Decreased hepatic expression of S6K improved glucose tolerance in NC and HFD mice, and enhanced systemic insulin sensitivity in liver, muscle, and adipose tissue in HFD mice, as demonstrated by hyperinsulinemic euglycemic clamp studies and insulin injections. How the liver communicates to these other key insulin target tissues remains to be explored, but decreased insulin and glucose levels can lead to improved insulin sensitivity in muscle and fat. Whether there are other mechanisms whereby the liver can communicate to distant tissues remains to be resolved.

In HFD mice, S6K remains activated despite the marked reduction in signaling through Akt. Furthermore, the effects of insulin to stimulate mTORC1/S6K were relatively preserved in liver tissue and hepatocytes from HFD/obese mice compared with Akt. The nature of this Akt independent pathway is of interest. For example, amino acids influence insulin action and activate mTORC1/S6K through class III PI3K (hVps34), providing a distinct Akt-independent pathway for S6K activation (26). Given the conditions of nutrient overload that exist in obesity, S6K activation by excess nutrients and/or insulin, independent of Akt, appear to provide an input to the lipogenic program through SREBP-1c, serving as a divergence point in the insulin signaling pathway responsible for selective, or mixed, hepatic insulin resistance.

In livers from L-S6K-KD mice there is a reduction in hepatic TG content and *de novo* lipogenesis. This is associated with decreased expression of SREBP-1c in both NC and HFD fed L-S6K-KD mice, consistent with the important role of SREBP-1c in liver lipogenesis. Circulating adipose tissue

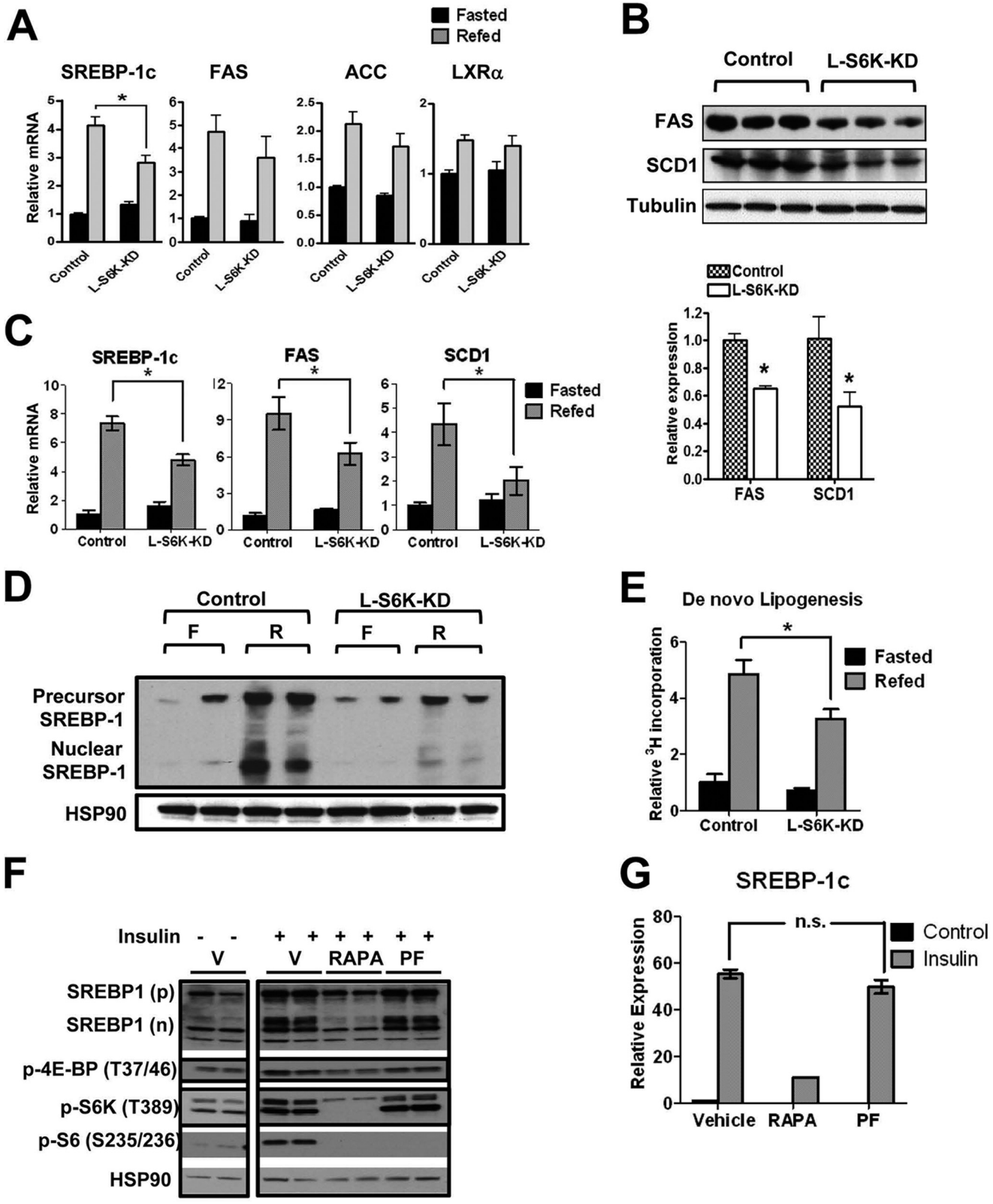

FIGURE 7. **S6K mediated regulation of lipogenic pathway is manifested in L-S6K-KD mice but not in isolated rat hepatocytes.** Relative amounts of mRNA for lipogenic genes in liver from HFD. *A*, relative amounts of mRNA for lipogenic genes in liver from HFD mice. *B*, protein expression of FAS and SCD1 in livers from HFD mice. *D*, immunoblot analysis for precusor and nuclear SREBP-1 protein levels in livers from NC mice. *E*, *de novo* lipogenesis measured by incorporation of radioactivity from ^3H_2O to the lipid fraction in livers from NC control and L-S6K-KD mice. *F*, immunoblot analysis for rat hepatocytes treated with inhibitors and insulin. Thirty minutes after incubation of cells with 10 nM rapamycin or 10 μM PF-4708671, 100 nM insulin was added for 24 h treatment. *RAPA*: rapamycin, *PF*: PF-4708671. *G*, SREBP-1c mRNA expression measured by q-PCR for samples treated as same as *F*.

derived FFA are also precursors to hepatic triglycerides and lower FFA levels in the L-S6K-KD mice could also contribute to the decreased steatosis. Less clear, is the precise mechanistic connection between S6K and increased SREBP-1c activity. The decreased SREBP-1c mRNA levels with S6K depletion appears to be independent of changes in LXRα activity, consistent with the view that insulin or nutrient stimulation of S6K is the input signal to SREBP-1c. We also find reduced levels of the active/nuclear form of SREBP-1c protein with S6K depletion in whole liver from L-S6K-KD mice. Therefore, a likely possibility is that in the *in vivo* situation, depletion of S6 kinase leads to a decrease in SREBP-1c mRNA expression, resulting in the decrease in SREBP-1c protein expression, decreased target gene expression, and, ultimately, the decrease in *de novo* lipogenesis. The mechanisms for this decrease in SREBP-1c expression are of interest, but remain unclear. Our *in vitro* studies using isolated rat hepatocytes show that chemical inhibition of S6 kinase does not decrease SREBP-1c expression. These latter results are fully consistent with an earlier report by Li *et al.*, who found that the mTOR inhibitor rapamycin blocks insulin induction of SREBP-1c, whereas, a small molecule inhibitor of S6 kinase did not, indicating the presence of a pathway downstream of mTORC1, distinct from S6 kinase, with input into SREBP-1c (17). One should note that the studies by Li *et al.*, as well as those shown in isolated hepatocytes in Fig. 7*F* of the current report, were performed *in vitro* after acute treatment, whereas, our *in vivo* studies utilized liver tissues after chronic siRNA-mediated knockdown. It seems possible that the partial decrease of S6 kinase activity achieved over the long term in our *in vivo* experiments links to regulation of lipogenesis through an indirect mechanism. Since nutrients, such as amino acids, can also stimulate S6 kinase signaling *in vivo*, perhaps the *in vivo* setting in which the liver is exposed to nutrient flow creates a pathway whereby the S6 kinase effects are manifested. Clearly, future studies of this possible mechanism are warranted.

Taken together, our results highlight the importance of hepatic S6K in the generation of insulin resistance and hepatic steatosis. Thus, even though insulin signaling through Akt is markedly reduced in the insulin resistant obese liver, S6K activity is still robustly activated, indicating Akt-independent inputs into S6K. We show that hepatic specific depletion of S6K interrupts its feedback inhibition of IRS, leading to enhanced insulin action in the NC and HFD/obese L-S6K-KD mouse. The present studies also demonstrate that hepatic lipogenesis is fully responsive to insulin stimulation in the obese/HFD mouse model, whereas, liver-specific S6K knockdown attenuated this lipogenic program by impairing SREBP-1c activation. In this way, S6K can integrate multiple inputs and serves as a key molecule in mediating mixed insulin resistance in livers from obese animals. These findings raise the possibility that hepatic S6K may be a potential therapeutic target in metabolic diseases.

Acknowledgments—We thank Jachelle M. Ofrecio and Sarah Nalbandian for help with animal maintenance and Elizabeth J. Hansen for editorial assistance.

REFERENCES

1. Brown, M. S., and Goldstein, J. L. (2008) Selective versus total insulin resistance: a pathogenic paradox. *Cell Metab.* **7,** 95–96
2. Hegarty, B. D., Bobard, A., Hainault, I., Ferré, P., Bossard, P., and Foufelle, F. (2005) Distinct roles of insulin and liver X receptor in the induction and cleavage of sterol regulatory element-binding protein-1c. *Proc. Natl. Acad. Sci. U.S.A.* **102,** 791–796
3. Leavens, K. F., Easton, R. M., Shulman, G. I., Previs, S. F., and Birnbaum, M. J. (2009) Akt2 is required for hepatic lipid accumulation in models of insulin resistance. *Cell Metab* **10,** 405–418
4. Biddinger, S. B., Hernandez-Ono, A., Rask-Madsen, C., Haas, J. T., Alemán, J. O., Suzuki, R., Scapa, E. F., Agarwal, C., Carey, M. C., Stephanopoulos, G., Cohen, D. E., King, G. L., Ginsberg, H. N., and Kahn, C. R. (2008) Hepatic insulin resistance is sufficient to produce dyslipidemia and susceptibility to atherosclerosis. *Cell Metab.* **7,** 125–134
5. Ma, X. M., and Blenis, J. (2009) Molecular mechanisms of mTOR-mediated translational control. *Nat. Rev. Mol. Cell Biol.* **10,** 307–318
6. Krebs, M., Brehm, A., Krssak, M., Anderwald, C., Bernroider, E., Nowotny, P., Roth, E., Chandramouli, V., Landau, B. R., Waldhäusl, W., and Roden, M. (2003) Direct and indirect effects of amino acids on hepatic glucose metabolism in humans. *Diabetologia* **46,** 917–925
7. Um, S. H., Frigerio, F., Watanabe, M., Picard, F., Joaquin, M., Sticker, M., Fumagalli, S., Allegrini, P. R., Kozma, S. C., Auwerx, J., and Thomas, G. (2004) Absence of S6K1 protects against age- and diet-induced obesity while enhancing insulin sensitivity. *Nature* **431,** 200–205
8. Khamzina, L., Veilleux, A., Bergeron, S., and Marette, A. (2005) Increased activation of the mammalian target of rapamycin pathway in liver and skeletal muscle of obese rats: possible involvement in obesity-linked insulin resistance. *Endocrinology* **146,** 1473–1481
9. Tremblay, F., Gagnon, A., Veilleux, A., Sorisky, A., and Marette, A. (2005) Activation of the mammalian target of rapamycin pathway acutely inhibits insulin signaling to Akt and glucose transport in 3T3-L1 and human adipocytes. *Endocrinology* **146,** 1328–1337
10. Zick, Y. (2004) Uncoupling insulin signaling by serine/threonine phosphorylation: a molecular basis for insulin resistance. *Biochem. Soc. Trans.* **32,** 812–816
11. Radimerski, T., Montagne, J., Hemmings-Mieszczak, M., and Thomas, G. (2002) Lethality of Drosophila lacking TSC tumor suppressor function rescued by reducing dS6K signaling. *Genes Dev.* **16,** 2627–2632
12. Harrington, L. S., Findlay, G. M., and Lamb, R. F. (2005) Restraining Pl3K: mTOR signaling goes back to the membrane. *Trends Biochem. Sci.* **30,** 35–42
13. Brown, N. F., Stefanovic-Racic, M., Sipula, I. J., and Perdomo, G. (2007) The mammalian target of rapamycin regulates lipid metabolism in primary cultures of rat hepatocytes. *Metabolism* **56,** 1500–1507
14. Porstmann, T., Santos, C. R., Griffiths, B., Cully, M., Wu, M., Leevers, S., Griffiths, J. R., Chung, Y. L., and Schulze, A. (2008) SREBP activity is regulated by mTORC1 and contributes to Akt-dependent cell growth. *Cell Metab.* **8,** 224–236
15. Baquet, A., Lavoinne, A., and Hue, L. (1991) Comparison of the effects of various amino acids on glycogen synthesis, lipogenesis and ketogenesis in isolated rat hepatocytes. *Biochem. J.* **273,** 57–62
16. Le Bacquer, O., Petroulakis, E., Paglialunga, S., Poulin, F., Richard, D., Cianflone, K., and Sonenberg, N. (2007) Elevated sensitivity to diet-induced obesity and insulin resistance in mice lacking 4E-BP1 and 4E-BP2. *J. Clin. Invest.* **117,** 387–396
17. Li, S., Brown, M. S., and Goldstein, J. L. (2010) Bifurcation of insulin signaling pathway in rat liver: mTORC1 required for stimulation of lipogenesis, but not inhibition of gluconeogenesis. *Proc. Natl. Acad. Sci. U.S.A.* **107,** 3441–3446
18. Yecies, J., Zhang, H., Menon, S., Liu, S., Yecies, D., Lipovsky, A., Gorgun, C., Kwiatkowski, D., Hotamisligil, G., Lee, C.-H., and Manning, B. (2011) Akt stimulated hepatic SREBP1c and lipogenesis through parallel mTORC1-dependent and independent pathways. *Cell Metabolism* **14,** 21–32
19. Peterson, T., Sengupta, S., Harris, T., Carmack, A., Kang, S., Balderas, E., Guertin, D., Madden, K., Carpenter, A., Finck, B., and Sabatini, D. (2011)

mTOR complex 1 regulates lipin 1 localization to control the SREBP pathway. *Cell* **146,** 408–420
20. Snyder, R. O., Miao, C. H., Patijn, G. A., Spratt, S. K., Danos, O., Nagy, D., Gown, A. M., Winther, B., Meuse, L., Cohen, L. K., Thompson, A. R., and Kay, M. A. (1997) Persistent and therapeutic concentrations of human factor IX in mice after hepatic gene transfer of recombinant AAV vectors. *Nat. Genet.* **16,** 270–276
21. Oh, D. Y., Talukdar, S., Bae, E. J., Imamura, T., Morinaga, H., Fan, W., Li, P., Lu, W. J., Watkins, S. M., and Olefsky, J. M. (2010) GPR120 is an omega-3 fatty acid receptor mediating potent anti-inflammatory and insulin-sensitizing effects. *Cell* **142,** 687–698
22. Yoshizaki, T., Milne, J. C., Imamura, T., Schenk, S., Sonoda, N., Babendure, J. L., Lu, J. C., Smith, J. J., Jirousek, M. R., and Olefsky, J. M. (2009) SIRT1 exerts anti-inflammatory effects and improves insulin sensitivity in adipocytes. *Mol. Cell Biol.* **29,** 1363–1374
23. Keshwani, M. M., and Harris, T. K. (2008) Kinetic mechanism of fully activated S6K1 protein kinase. *J. Biol. Chem.* **283,** 11972–11980
24. Jiang, G., Li, Z., Liu, F., Ellsworth, K., Dallas-Yang, Q., Wu, M., Ronan, J., Esau, C., Murphy, C., Szalkowski, D., Bergeron, R., Doebber, T., and Zhang, B. B. (2005) Prevention of obesity in mice by antisense oligonucleotide inhibitors of stearoyl-CoA desaturase-1. *J. Clin. Investig.* **115,** 1030–1038
25. Aguilar, V., Alliouachene, S., Sotiropoulos, A., Sobering, A., Athea, Y., Djouadi, F., Miraux, S., Thiaudière, E., Foretz, M., Viollet, B., Diolez, P., Bastin, J., Benit, P., Rustin, P., Carling, D., Sandri, M., Ventura-Clapier, R., and Pende, M. (2007) S6 kinase deletion suppresses muscle growth adaptations to nutrient availability by activating AMP kinase. *Cell Metab.* **5,** 476–487
26. Nobukuni, T., Joaquin, M., Roccio, M., Dann, S. G., Kim, S. Y., Gulati, P., Byfield, M. P., Backer, J. M., Natt, F., Bos, J. L., Zwartkruis, F. J., and Thomas, G. (2005) Amino acids mediate mTOR/raptor signaling through activation of class 3 phosphatidylinositol 3OH-kinase. *Proc. Natl. Acad. Sci. U.S.A.* **102,** 14238–14243
27. Deleted in proof